Simulation Study for a New Magnetic Induction Tomography Coil System with Weakly Perturbing in Conducting Background

Ziyi Zhang*, Peiguo Liu-*IEEE Member*, Dongming Zhou, Liang Zhang, and Hengdong Lei

Abstract— **Biomedical magnetic induction tomography (MIT) aims to reconstruct the passive electrical properties within biological tissues, especially the electrical conductivity. A weak perturbation inside a conducting object is put in the improved MIT coil system which uses the two-arm Archimedean spiral coil as the excitation coil and the circular coil as the receiver coil. The forward problem for this model is calculated by three-dimension electromagnetic simulation experiments. Under the different simulation conditions, the phase shift of voltage induced in the receiver coil is compared with that for the common model using the circular coil as the excitation and receiver coil. The results show that the sensitivity to the improved model is much higher than that to the common model except for the case that the perturbation appears in *y*-axis, which effectively confirms the previous conclusions and indicates that the improved coil system has the potential advantage for MIT image reconstruction.**

I. INTRODUCTION

Biological tissues have three important electromagnetic parameters called the passive electrical property (PEP) which could reflect their physiological states, namely the dielectric permittivity, the magnetic permeability and the electrical conductivity. Changes of the PEP in biological tissues are the natural concomitants of many pathological processes. For instance, for the patients who are suffering from the brain edema or the hemorrhagic cerebral stroke, the values of electrical conductivity of the lesion are often larger than those of the surrounding normal tissues [1, 2].

Biomedical magnetic induction tomography (MIT) is an emerging kind of functional and dynamic imaging modality aiming at mapping the internal electrical conductivity of biological tissues. It is an attractive technique due to its non-invasive and contactless feature [3, 4]. The imaging could be realized by rotating a pair of excitation and receiver coils around the object under investigation to measure a set of signals (e.g., voltages) induced in the receiver coil and then applying several reconstructed algorithms to map the electrical conductivity distribution of the object from the received data. In MIT the coil system plays a vital role, because the reconstructed image quality is greatly influenced by its sensitivity [5–8]. In order to improve the coil system sensitivity, the two-arm Archimedean spiral coil (TAASC) is introduced into MIT as the excitation coil [9]. The TAASC is constructed with two Archimedean planar spirals which are connected in the opposite direction. This anti-symmetric configuration helps to counteract the primary excitation magnetic fields emitted by itself [9–11]. Fig. 1 shows the TAASCs with different numbers of turns.

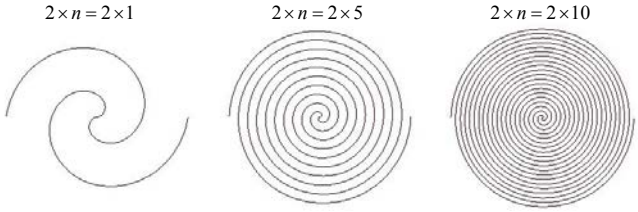

Figure 1. TAASCs with different numbers of turns (n = 1, 5, 10).

The performance for the improved MIT coil system with a conducting perturbation in the empty space has been studied, and shows that it is better in sensitivity than that for the common coil system which uses the circular coil as the excitation and receiver coil [9]. In this paper, the weak perturbation in the conducting background is considered. The forward problems for the improved and common coil systems are calculated by three-dimension electromagnetic simulation software CST EM STUDIO (CST AG). The phase shifts of received voltage for the improved and common coil systems are simulated when the position, size and electrical conductivity of the perturbation are changed.

II. METHODS

A. Forward Problem in MIT

Solving the MIT forward problem is a precondition for the image reconstruction. Actually, the forward problem in MIT is an eddy-current problem, which follows the time-harmonic Maxwell equations in frequency domain:

$$\begin{aligned} \nabla\times\frac{1}{\mu}\boldsymbol{B} &= \sigma\boldsymbol{E}+j\omega\varepsilon\boldsymbol{E}+\boldsymbol{J}_s \\ \nabla\times\boldsymbol{E} &= -j\omega\boldsymbol{B} \\ \nabla\bullet\boldsymbol{B} &= 0 \\ \nabla\bullet\varepsilon\boldsymbol{E} &= \rho \end{aligned} \tag{1}$$

where $\boldsymbol{E}$ and $\boldsymbol{B}$ are the electric field intensity and magnetic induction intensity respectively, $\boldsymbol{J}_s$ and ω are the electric

This work was supported by the National Natural Science Foundation (No. 61372029) from People's Republic of China, the Specialized Research Fund for the Doctoral Program of Higher Education (No. 20114307110022) from Ministry of Education of the People's Republic of China, and the Innovation Fund for Doctoral Candidate (No. B130205) from National University of Defense Technology. *Asterisk indicates corresponding author.*

Z. Zhang, L. Zhang and H. Lei are with the College of Science, National University of Defense Technology, Changsha, Hunan 410073, China, and also with the State Key Laboratory of Complex Electromagnetic Environmental Effects on Electronics & Information System, National University of Defense Technology, Changsha, Hunan 410073, China (e-mail: ziyizhang@nudt.edu.cn; liangzhang@nudt.edu.cn; lhdandkt@gmail.com).

P. Liu and D. Zhou are with the State Key Laboratory of Complex Electromagnetic Environmental Effects on Electronics & Information System, National University of Defense Technology, Changsha, Hunan 410073, China (e-mail: peiguo_Liu@hotmail.com; dmzhou@nudt.edu.cn).

current density and angular frequency of the excitation source respectively, ε, μ, σ and ρ are the dielectric permittivity, the magnetic permeability, the electrical conductivity and the electric charge density respectively, and j is the imaginary unit.

The displacement current could be neglected in the condition of low frequency due to its small magnitude in comparison with that of the conduction current. When the excitation frequency is up to 10 MHz, however, the displacement current is significant and non-ignorable [12].

The finite element method [12, 13] or the finite difference method [14, 15] could be used to solve the forward problem in MIT. After obtaining $\boldsymbol{E}$, the voltage V induced in the receiver coil could be evaluated by:

$$V = \oint \boldsymbol{E} \cdot d\boldsymbol{l} \tag{2}$$

where $d\boldsymbol{l}$ is the vector length element of the receiver coil.

Changes $\Delta\sigma$ of the electrical conductivity in the region of interest would lead to a perturbation $\Delta\phi$ in phase of the signal induced in the receiver coil. This makes an approximately linear relationship as below [3]:

$$\Delta\phi \propto \omega\Delta\sigma \tag{3}$$

In this paper, the forward problem in MIT is solved by three-dimension electromagnetic simulation software CST EM STUDIO. The computation is in frequency domain and the fullwave solver equation is used.

B. Simulation Model

The sketch map for the improved coil system is shown in Fig. 2. The excitation coil is a TAASC and the receiver coil is a circular coil, and they are placed coaxially. The conducting object which contains the electrical conductivity perturbation could be put in the space between the two coils.

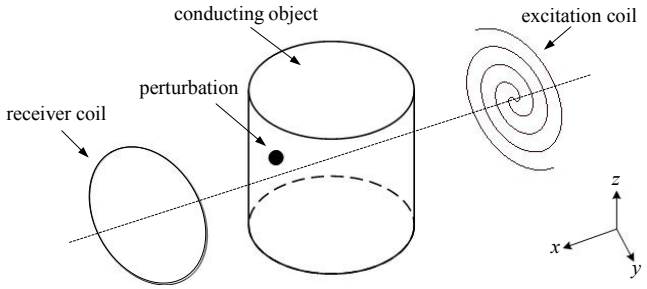

Figure 2. Sketch map for improved coil system.

For the sake of simplification, the conducting object model is treated as a cylinder and the perturbation model is treated as a small sphere. The wire diameters for the excitation coil and the receiver coil are ignored. Fig. 3 describes the simulation model of electromagnetic calculation. The magnitude and frequency of the sinusoidal excitation current are I and f, respectively. The receiver coil is a circular coil and its radius is r_0. When the excitation coil is a TAASC, its maximum outer radius and number of turns are r_0 and $2 \times n$, respectively. When the excitation coil is the circular coil, its radius is r_0 as well. The spherical perturbation is positioned at (x, y, z), with the radius of r. The electrical conductivities of the conducting object and perturbation are σ_1 and σ_2, respectively. The values of simulated parameters are listed in Table 1.

TABLE I. VALUES OF SIMULATED PARAMETERS

Parameters	I	f	n	r_0
Values	1 A	10 MHz	1	50 mm
Parameters	r	R	h	d
Values	5 mm	60 mm	120 mm	220 mm
Parameters	σ_1	σ_2	–	–
Values	1 S/m	2 S/m	–	–

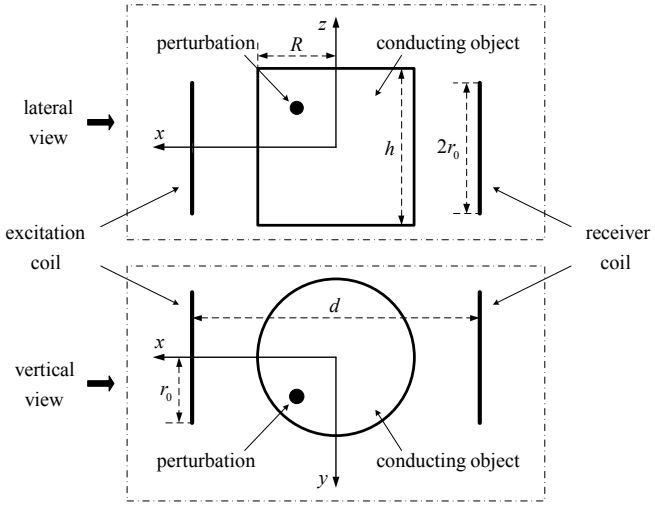

Figure 3. Simulation model for electromagnetic calculation.

III. RESULTS

A. Coil System Sensitivity versus Position of Perturbation

The phase shifts of voltage induced in the receiver coil versus the positions of perturbation for the improved and common coil systems are shown respectively in Fig. 4. The perturbation is limited to move on the coordinate axis. The variation ranges for x, y, z are all –40 mm to 40 mm. The phase shift is expressed as $\Delta\phi$.

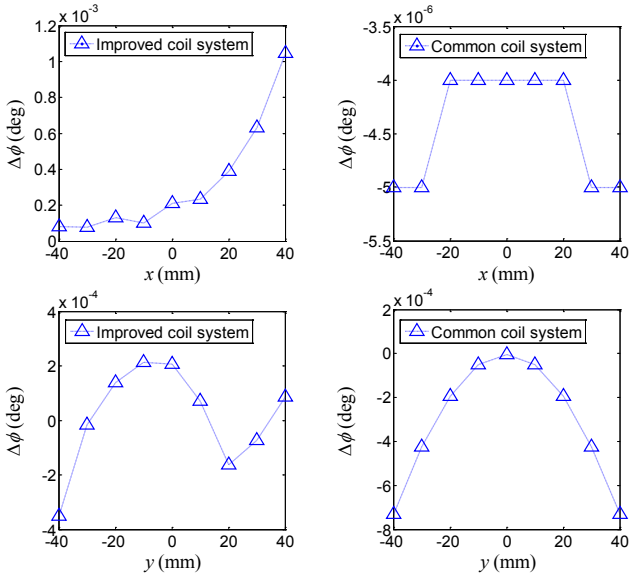

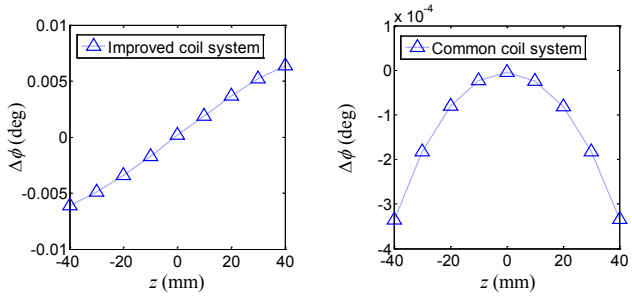

Figure 4. Phase shifts of the received voltage versus x, y and z position of the perturbation for the improved and common coil systems.

B. *Coil System Sensitivity versus Size of Perturbation*

Fig. 5 shows the phase shifts of voltage induced in the receiver coil versus the sizes of perturbation for the improved and common coil systems, respectively. Three kinds of spherical perturbation with different radius are chosen, namely $r = 5$ mm, 10 mm and 15mm. The volumes of the perturbation are approximately 0.5 ml, 4 ml and 14 ml accordingly. The perturbation is positioned at the point ($x = 0$, $y = 0$, $z = 0$) and the point (x =30 mm, $y = 30$ mm, $z = 30$ mm) which is treated as an arbitrary point.

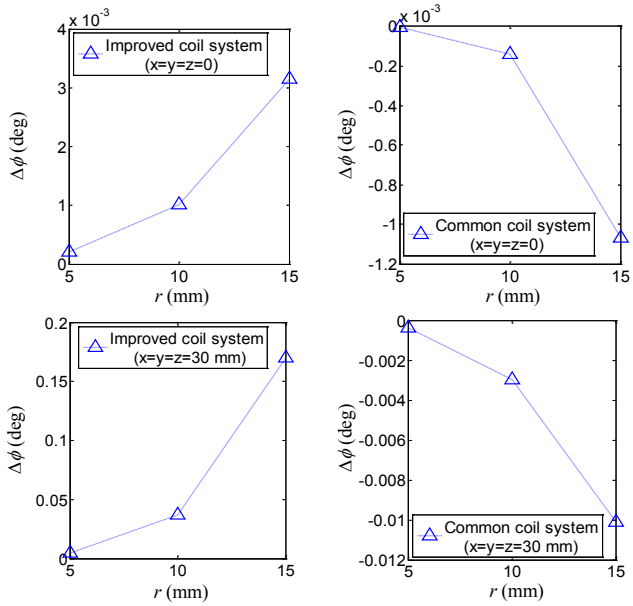

Figure 5. Phase shifts of the received voltage versus sizes of the perturbation for the improved and common coil systems when locations of perturbation are ($x = 0$, $y = 0$, $z = 0$) and ($x = 30$ mm, $y = 30$ mm, $z = 30$ mm).

C. *Coil System Sensitivity versus Electrical Conductivity of Perturbation*

Fig. 5 shows the phase shifts of voltage induced in the receiver coil versus the electrical conductivities of perturbation for the improved and common coil systems, respectively. The locations of the small spherical perturbation are at the points ($x = 0$, $y = 0$, $z = \pm 30$ mm), ($x = \pm 30$ mm, $y = 0$, $z = 0$), ($x = 0$, $y = \pm 30$ mm, $z = 0$), ($x = 0$, $y = 0$, $z = 0$) in the coordinate axis and the point ($x = 30$ mm, $y = 30$ mm, $z = 30$ mm). The electrical conductivity of perturbation changes from 1 S/m to 5 S/m.

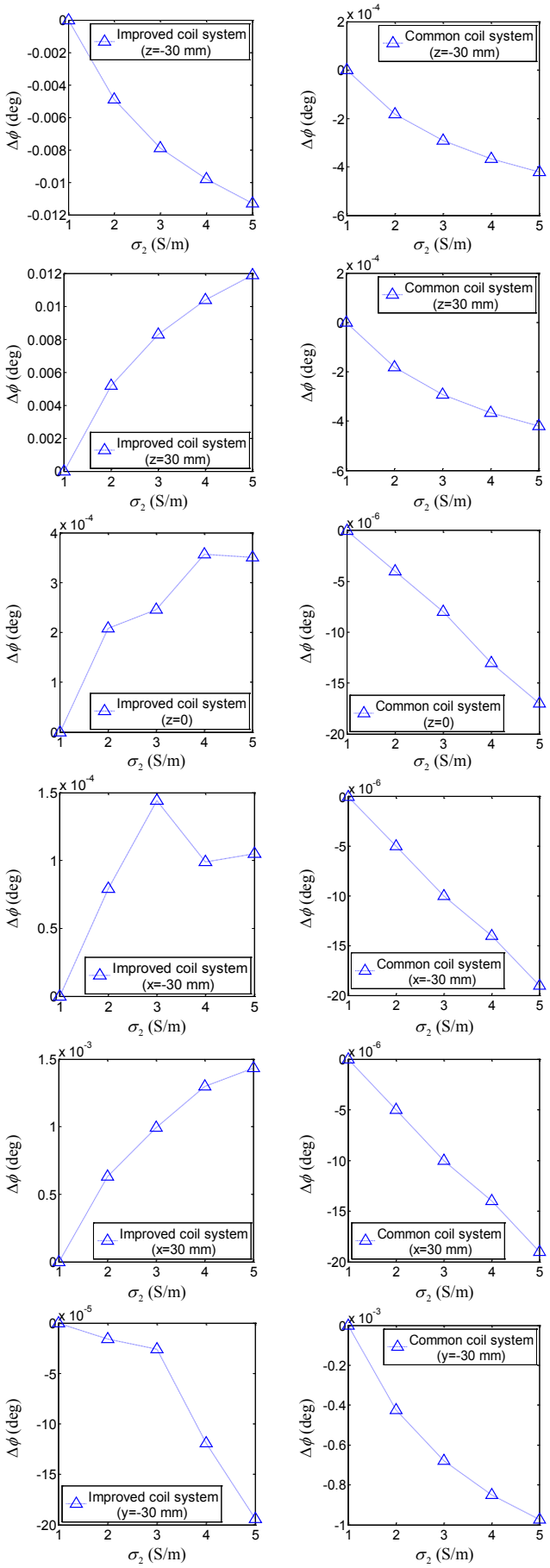

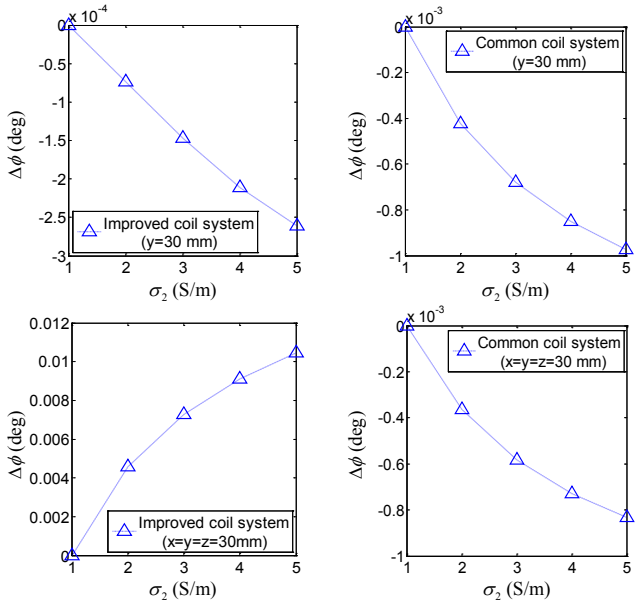

Figure 6. Phase shifts of the received voltage versus electrical conductivities of the perturbation for the improved and common coil systems when the locations of perturbation are at ($x = 0$, $y = 0$, $z = \pm 30$ mm), ($x = 0$, $y = \pm 30$ mm, $z = 0$), ($x = \pm 30$ mm, $y = 0$, $z = 0$), ($x = 0$, $y = 0$, $z = 0$) and ($x = 30$ mm, $y = 30$ mm, $z = 30$ mm).

IV. Discussions and Conclusions

It could be seen from Fig. 4 that the sensitivity to the improved coil system is much higher than that to the common coil system in x and z directions, and the sensitivity for the improved coil system is modified approximately two orders compared with that for the common coil system. However, the sensitivity in y direction to the improved coil system is unsatisfactory. Theoretically, the response shape in y direction for the improved coil system should be anti-symmetric to the zero. Due to the calculation errors of software, this shape simulated is slight deformation. In addition, the variation trend for the simulated curves is mainly in agreement with the previous studies which only take into account the conducting perturbation in the empty space [9].

In Fig. 5 the phase shift of voltage induced in the receiver coil would become large with the increasing of the perturbation size. The sensitivity to the improved coil system is a bit higher than that to the common coil system in the position of original point, while dramatically at the point chosen as an arbitrary point (x = 30 mm, y = 30 mm, z = 30 mm).

Fig. 6 further verifies the results of Fig. 4. It demonstrates that the performance for the improved coil system is superior to that for the common coil system in the x and z directions no matter how the position and electrical conductivity of the perturbation change. In the y direction the sensitivity versus electrical conductivity for the improved is approximately one magnitude lower than that for the common coil system. To the arbitrary position which is not chosen in the coordinate axis, the sensitivity for the improved coil system exceeds that for the common coil system by more than an order of magnitude. Fig. 6 also confirms the validity of (3), showing linearity basically.

According to above results of simulation, the improved MIT coil system could well improve the sensitivity in most situations except for the case that conducting perturbation appears in y-axis. Therefore, this new type of coil system has the potential application for MIT. The study of this paper are ideal and simplified. More accurate and practical calculation experiments are needed to further research.

References

[1] H. Scharfetter, R. Casañas and J. Rosell, "Biological tissue characterization by magnetic induction spectroscopy (MIS): requirements and limitations," *IEEE Trans. Biomed. Eng.*, vol. 50, pp. 870–880, Jul. 2003.

[2] B. Dekdouk, "Image reconstruction of low conductivity material distribution using magnetic induction tomography," Ph.D. dissertation, Dept. Elect. Electron. Eng., Manchester Univ., Manchester, UK, 2011.

[3] H. Griffiths, "Magnetic induction tomography," *Meas. Sci. Technol.*, vol. 12, pp. 1126–1131, Aug. 2001.

[4] H.-Y. Wei and M. Soleimani, "Electromagnetic tomography for medical and industrial applications: challenges and opportunities," *Proc. IEEE*, vol. 101, pp. 27–46, Mar. 2013.

[5] A. J. Peyton, Z. Z. Yu, G. Lyon, S. Al-Zeibak, J. Ferreira, J. Velez, F. Linhares, A. R. Borges, H. L. Xiong, N. H. Saunders and M. S. Beck, "An overview of electromagnetic inductance tomography: description of three different systems," *Meas. Sci. Technol.*, vol. 7, pp. 261–271, Mar. 1996.

[6] H. Griffiths, W. R. Stewart and W. Gough, "Magnetic induction tomography: a measuring system for biological tissues," *Ann. N.Y. Acad. Sci.*, vol. 873, pp. 335–345, Apr. 1999.

[7] S. Watson, C. H. Igney, O. Dössel, R. J. Williams and H. Griffiths, "A comparison of sensors for minimizing the primary signal in planar-array magnetic induction tomography," *Physiol. Meas.*, vol. 26, pp. S319–S331, Apr. 2005.

[8] H. Scharfetter, R. Merwa and K. Pilz, "A new type of gradiometer for the receiving circuit of magnetic induction tomography (MIT)," *Physiol. Meas.*, vol. 26, pp. S307–S318, Apr. 2005.

[9] Z. Zhang, P. Liu, D. Zhou and H. Lei, "Biomedical magnetic induction using two-arm Archimedean spiral coil: a feasibility study," in *Proc. 13th IEEE Int. Conf. Bioinformatics and Bioengineering*, Chania, Greece, 2013.

[10] Z. Zhang, H. Lei, P. Liu and D. Zhou, "Sensitivity study for improved magnetic induction tomography (MIT) coil system," in *Proc. 2013 Int. Symp. Antennas and Propagation*, Nanjing, China, 2013, pp. 1317–1320.

[11] Z. Zhang, P. Liu, L. Ding and L. Zhang, "A new type of excitation coil for measurement of liver iron overload by magnetic induction method," in *Proc. 5th Int. Conf. Biomedical Engineering and Informatics*, Chongqing, China, 2012, pp. 679–683.

[12] M. Zolgharni, P. D. Ledger and H. Griffiths, "Forward modelling of magnetic induction tomography: a sensitivity study for detecting haemorrhagic cerebral stroke," *Med. Biol. Eng. Comput.*, vol. 47, pp. 1301–1313, Dec. 2009.

[13] K. Hollaus, C. Magele, R. Merwa and H. Scharfetter, "Fast calculation of the sensitivity matrix in magnetic induction tomography by tetrahedral edge finite elements and the reciprocity theorem," *Physiol. Meas.*, vol. 25, pp. 159–168, Feb. 2004.

[14] H. Scharfetter, P. Riu, M. Populo and J. Rosell, "Sensitivity maps for low-contrast perturbations within conducting background in magnetic induction tomography," *Physiol. Meas.*, vol. 23, pp. 195–202, Feb. 2002.

[15] M. Qin, Y. Wang, X. Hu, M. Jiao, W. Liang, H. Zhang and H. Wang, "Study of MIT phase sensitivity for detecting a brain edema based on FDTD method," in *Proc. 1st Int. Conf. Bioinformatics and Biomedical Engineering*, Wuhan, China, 2007, pp. 660–663.